



7th Asian-Pacific Conference on Aerospace Technology and Science, 7th APCATS 2013

A ghost cell method for turbulent compressible viscous flows on adaptive Cartesian grids

O. Hu^{a,*}, N. Zhao^a, J. M. Liu^a

^a*Nanjing University of Aeronautics and Astronautics, Nanjing, 210016, China*

Abstract

The aim of this paper is to present a new ghost cell turbulent wall boundary condition to simulate high Reynolds number compressible viscous flows on adaptive Cartesian grids. A pure Cartesian grid has been established with the bodies embedded into the grid. Instead of cut cell approach, a ghost cell immersed boundary method has been applied and a wall function model is devised to treat turbulent wall boundary conditions. The law-of-the-wall is employed to define primitive variables and turbulent properties at the ghost cells. Furthermore, the turbulent variables at the near wall cells and boundary cells are modified by using wall function model. In the frame of adaptive Cartesian grids, a cell-centered, second-order accurate finite volume solver has been developed for predicting turbulent flow fields. The robustness and the accuracy of the methodology have been validated versus well documented turbulent flow test problems, such as transonic flow past a RAE2822 airfoil and supersonic flow past a circle cylinder. The obtained results show the effectivity and reliability of the new numerical methods.

© 2013 The Authors. Published by Elsevier Ltd. Open access under [CC BY-NC-ND license](#).
Selection and peer-review under responsibility of the National Chiao Tung University

Keywords: ghost cell method; immersed boundary method; wall function; adaptive Cartesian grid; turbulent flow

1. Introduction

With the development of computer science and numerical method, Cartesian grids become one of the popular mesh generation methods and can be considered for real, large scale numerical simulations. Traditional body-fitted methods are time-consuming and need a high level of expertise especially for complex geometries. However, Cartesian grid methods are thought to be automation and flexibility in grid generation, especially when the

* Corresponding author. Tel.: +86-025-84892628; fax: +86-025-84892628.
E-mail address: huou_nuaa@nuaa.edu.cn

adaptive mesh refinement (AMR) technique is coupled with them. They could be ease and speed, even automated to generate mesh for complex geometries, such as multi-scale problems and moving boundary problems.

The main difficulty in using adaptive Cartesian grids for simulating flow-fields is the boundary treatment of high Reynolds number turbulent compressible flow problems. Many earlier Cartesian grids based flow solvers [1-2] employed “Cartesian cut-cell” approach to deal the intersection between the Cartesian cells and the body surface. But, this method would form a cell with arbitrary shape and make the data structure more complicated. In recent years, another approach named as “immersed boundary method (IBM)” became more and more popular in dealing the boundary conditions for Cartesian grid methods. Compared with “Cartesian cut-cell” method, the main advantage of the IBM consists in avoiding complex geometrical algorithms to intersect the Cartesian cells with the body surface. **The IBM just need enforce the wall condition indirectly through the use of force terms**, so it keeps the advantage of automated grid generation of Cartesian grids.

Most of the IBM applications were available in simulating incompressible flows [3-4], they did very well in treating fluid-structure interaction and moving boundary problems. For compressible flows, a number of methods like the approach of IBM were available for Euler [5-6] and laminar flows [7-8], such as the “ghost-cell method” for inviscid flows developed by A.Dadone [5] and the “embedded boundary method” for laminar flows presented by D.Marshall [7]. However, there were some technique difficulties in predicting compressible turbulent flows with Cartesian grids. In references [9-10], some turbulent results were presented by using very fine mesh generated near the wall. But compared to body-fitted grid methods the he number of grid cells is **huger**. Some attempts were employed to decrease the excessive number of grid cells. One approach developed by Kamatsuchi [11] was to use the idea of sub-grid points in the boundary layer region to model turbulent boundary layers. Another way to avoid lager meshes in the boundary layer region was to use the wall model to represent turbulent boundary conditions in the case of turbulent flows at high Reynolds numbers. Some pioneer works by G. Kalitzin and G. Iaccarino [12-13] focused on coupling a logarithmic law of the wall with the IBM to simulate turbulent flows. Lee.J [14] developed a turbulent wall function based viscous Cartesian grid method in his doctoral thesis. F. Capizzano [15] adopted a two-layer wall modeling to correctly control the turbulent quantities at the immersed boundary surfaces.

In this paper, a novel cell-centered, second-order accurate finite volume solver has been developed for solving high Reynolds compressible viscous flows on adaptive Cartesian grids. In order to treat the non-body-conforming wall boundary conditions, a ghost cell immersed boundary method coupled with wall function model is devised, which is the major obstacle in solving Reynolds average Navier-Stokes(RANS) equations and turbulence models in conjunction with Cartesian grids. The law-of-the-wall has been applied to define the eddy viscosity, turbulent kinetic energy and specific dissipation of turbulence at the ghost cells. Furthermore, the primitive variables of the ghost cell were derived from the fundamental assumptions of wall function boundary conditions.

2. Governing equations and numerical methods

2.1. Governing equations

Two-dimensional compressible flows are governed by the Favre Reynolds averaged Navier-Stokes (RANS) equations. In an integral form, the RANS equations can be written as:

$$\frac{\partial}{\partial t} \int_{\Omega} W d\Omega + \oint_{\partial\Omega} (\mathbf{F}_c - \mathbf{F}_v) d\mathbf{S} = 0 \quad (1)$$

where \mathbf{W} is the vector of conserved variables, \mathbf{F}_c and \mathbf{F}_v are inviscid and viscous flux vector respectively[16]. Expressing the above equations over an arbitrary control volume Ω_i , the following semi-discrete form can be obtained:

$$\frac{d\mathbf{W}}{dt} = -\frac{1}{\Omega_i} \sum_{m=1}^{N_f} (\mathbf{F}_c - \mathbf{F}_v)_m \Delta S_m \quad (2)$$

In the above equation, m refers to the interface between the cell I and its neighboring cell J , N_f denotes the number of the interfaces of the control volume and ΔS_m is the area of the m interface. The solution is updated using

a LU-SGS implicit time integration procedure [17]. The two equation SST $k-\omega$ turbulence model developed by Menter [18] is implemented to handle turbulent flows.

2.2. Numerical methods

A cell-centered, second-order accurate finite volume method is used in order to solve equation (2). The convective flux vector of equation (2) is computed at the cell interface using the AUSM+ scheme developed by Liou [19], and the solution reconstruction procedure [16] is used to obtain second order accuracy. The diffusive flux vector is approximated by using 2nd order accurate central difference scheme.

The farfield boundary conditions considered in this work are based on simplified one-dimensional characteristics boundary conditions [16]. A ghost cell immersed boundary method, presented in section 4, is devised to treat turbulent wall boundary conditions.

2.3. Feature-based grid adaptation Numerical Methods

In the frame of adaptive Cartesian grids, a quadtree-based structure [1] is used to store the mesh information. The appealing advantage of tree-based data structure is the easy implementation of refinement or coarsening of cells, which makes the solution adaptations become a facile task. Sensors are employed to detect zones of appreciable flow activity. Since a criterion based on the divergence of velocity and the curl of velocity works the best [1], we will use the combination of those sensors, which expressed as follows:

$$\tau_{c_i} = |\nabla \times V| h_i^{\frac{r+1}{r}} \quad \tau_{d_i} = |\nabla \bullet V| h_i^{\frac{r+1}{r}} \quad (3)$$

where $I = 1, 2, \dots, N$, N being the total number of cells, $h_i = \sqrt[r]{\Omega_i}$ (Ω_i is the cell volume) represents the length scale of cell. The standard deviations of both parameters are computed as:

$$\sigma_c = \sqrt{\frac{\sum_{i=1}^N \tau_{c_i}^2}{N}}, \quad \sigma_d = \sqrt{\frac{\sum_{i=1}^N \tau_{d_i}^2}{N}} \quad (4)$$

Then the following conditions are used for grid adaptation.

- (1) if $\tau_{c_i} > \sigma_c$ or $\tau_{d_i} > \sigma_d$, cell I is flagged for refinement;
- (2) if $\tau_{c_i} < 0.3\sigma_c$ and $\tau_{d_i} < 0.1\cdot\sigma_d$, cell I is flagged for coarsening.

3. Wall function model

Wall function models are empirical relationships, which derived from the boundary layer theory and established on the six fundamental assumptions [20]. Spalding[21] suggested a unified valid for the log layer and the sublayer as well as the transition region. The form is given by:

$$y^+ = u^+ + e^{-\kappa y} \left[e^{\kappa y} - 1 - \kappa u^+ - \frac{(\kappa u^+)^2}{2} - \frac{(\kappa u^+)^3}{6} \right] \quad (5)$$

where y^+ and u^+ are defined as :

$$u^+ = \frac{u}{u_r}, \quad y^+ = \frac{\rho_w u_r y}{\mu_w}, \quad u_r = \sqrt{\frac{\tau_w}{\rho_w}} \quad (6)$$

In the above formulas u is the velocity parallel to the wall, y is coordinate direction normal to the wall. ρ_w , μ_w , τ_w are wall density, wall molecular viscosity and wall shear stress respectively. u_r means the friction velocity. The constants κ and B are taken as 0.41 and 5.5.

In order to treat the wall boundary condition, a ghost cell immersed boundary method is developed, based on the above wall function model and the fundamental assumptions, to define the flow variables at the ghost cells.

4. Ghost cell immersed boundary method

In the frame of ghost cell immersed boundary method, the geometry that is described by a closed polygon $\partial\Omega_w$ in two dimensions is overlapped onto a Cartesian grid. As shown in Fig. 1, the ray tracing technique based on the geometrical algorithms [22] is used to categorize the mesh into three kinds: flow cell (completely inside the fluid), boundary cell (intersect with wall boundary) and the rest solid cell (completely inside the solid). Meanwhile, the solid cell next to boundary cell is defined as ghost cell and flow cell next to boundary cell is named as near-wall-cell as shown in Fig. 1.

The wall function model, presented in section 3, is employed to define the turbulent wall boundary conditions at the ghost cells and to modify the turbulent properties at the near-wall-cells and boundary cells.

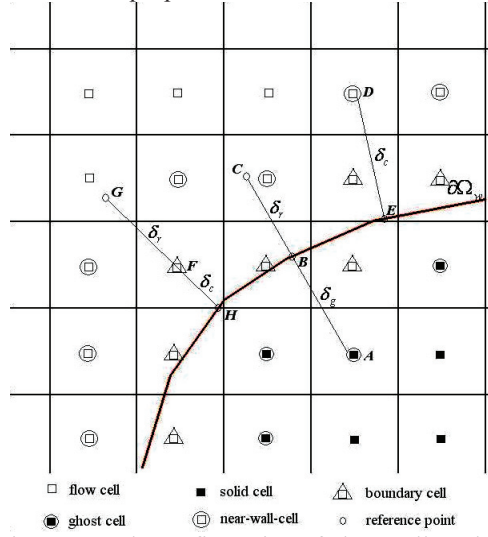


Fig.1 Example configuration of ghost cell method

4.1. Definition of primitive variables at the ghost cell

The primitive variables at the ghost cell are determined as following. As shown in Fig.1, consider the ghost cell A:

Firstly, find its reference point C, which is at the direction of line AB. The point B is the closest point on the body surface from the ghost cell A and the length of segment AB is δ_r . The length of segment BC is predetermined length, δ_r . (In this paper, δ_r is set to the length of boundary cell). Then, the primitive variables at the reference point are interpolated from the surrounding flow cells using the bilinear interpolation.

Secondly, using the primitive variables at the reference point, the tangential velocity and normal velocity V_{ref} at the reference point, and the density, molecular velocity at the wall can be obtained. Then, the wall shear stress τ_w and friction velocity u_* are obtained by solving equation (5) and (6) using Newton method.

Finally, according to the fundamental assumptions of wall function model [20], the shear stress is constant in the lower part of the boundary layer. Therefore, the shear stress at the ghost cell is set equal to the shear stress at the reference point, also equal to the wall shear stress τ_w . Meanwhile, assuming the total viscosity at the ghost cell is identical to that at the reference point. Then, the tangential velocity at the ghost cell is

$$V_{tg} \approx V_{ref} - \frac{\delta_r + \delta_g}{\mu_{ref} + \mu_{ref}} \tau_w \quad (7)$$

The normal velocity at the ghost cell satisfies the non-permeable wall boundary condition, that is

$$V_{Ng} = -\frac{\delta_g}{\delta_r} V_{Nref} \quad (8)$$

In the above equations, V_{Nref} and V_{Nng} represent the tangential and normal velocity at the reference point respectively. μ_{ref} and μ_{ng} are the molecular viscosity and eddy viscosity of the reference point respectively.

According to the fundamental assumptions of wall function model [20], the pressure is constant in the lower part of the boundary layer. That means the pressure at the ghost cell is identical to that at the reference point

$$P_g = P_{ref} \quad (9)$$

According to the fundamental assumptions of wall function model [20], the temperature profile in the lower part of the boundary layer satisfies the Crocco-Busemann equation. Then, the temperature at the ghost cell is expressed as

$$T_g = T_{ref} + \frac{r}{2} \frac{V_{Nref}^2 - V_{Ng}^2}{C_p} \quad (10)$$

Therefore, the density at the ghost cell can be obtained from the state law.

4.2. Specification and modification of turbulent properties

The SST $k - \omega$ turbulence model is employed to simulate turbulent flow. At the same time, a wall function model based turbulent wall boundary conditions are implemented. So the turbulent properties, such as the turbulent kinetic energy k , the specific dissipation of turbulence ω and the turbulent eddy viscosity μ_t , should be imposed on the ghost cells, also a modification of turbulent properties should be done at near-wall-cells and boundary cells.

According to the fundamental assumptions of wall function model [20], the shear stress is constant in the lower part of the boundary layer. Meanwhile, the relationship between molecular viscosity and turbulent eddy viscosity in the lower part of the boundary layer is expressed by taking derivation y^+ of u^+ [20]

$$\frac{\mu_t}{\mu_w} = \kappa e^{-x^B} \left[e^{ku^+} - 1 - \kappa u^+ - \frac{(ku^+)^2}{2} \right] \quad (11)$$

As shown in Fig.1, the sum of molecular viscosity and turbulent eddy viscosity is constant along the direction of the ghost cell A and its reference point E. Therefore, the turbulent eddy viscosity at the ghost cell yields to

$$\mu_{Ng} = \mu_{ref} + \mu_{Nref} - \mu_k \quad (12)$$

In the above equation, the molecular viscosity μ_g at the ghost cell and μ_{ref} at the reference point are obtained by using Sutherland's law [16]. The turbulent eddy viscosity μ_{Nref} at the reference point is obtained from the equation (11). The turbulent kinetic energy k and the specific dissipation of turbulence ω at the ghost cell are specified as follows [20]

$$\begin{aligned} \omega_i &= \frac{6\mu_w}{0.075\rho_w y^2} & \omega_o &= \frac{u_r}{\sqrt{C_\mu \kappa y}} & \omega &= \sqrt{\omega_i^2 + \omega_o^2} \\ k &= \frac{\omega \mu_i}{\rho} \end{aligned} \quad (13)$$

where ρ_w , μ_w represent wall density and wall molecular viscosity, y is coordinate direction normal to the wall, u_r means friction velocity calculated from wall function model, C_μ and κ are constants.

It's the same approach as used in the body-fitted grid methods [20], the turbulent properties should be modified at the near-wall-cells and boundary cells. As shown in Fig.1, for the near-wall-cells, the turbulent properties are calculated from the stored flow properties of themselves. However, turbulent properties at the boundary cells are calculated from their reference points the same as the approach of the ghost cells.

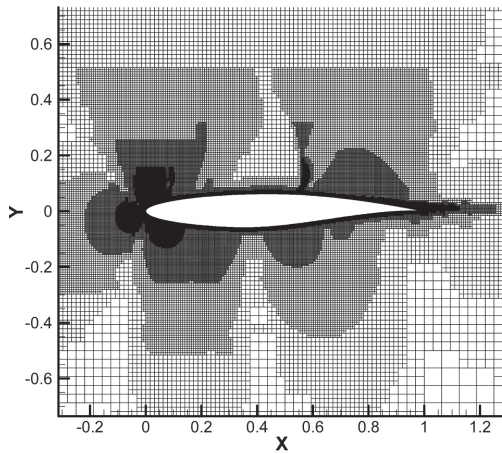
5. Results and Discussions

The proposed methodology has been applied to compute two-dimensional turbulent compressible viscous flows with adiabatic wall boundary conditions, including transonic flow over the RAE2822 airfoil and supersonic flow over the circle cylinder.

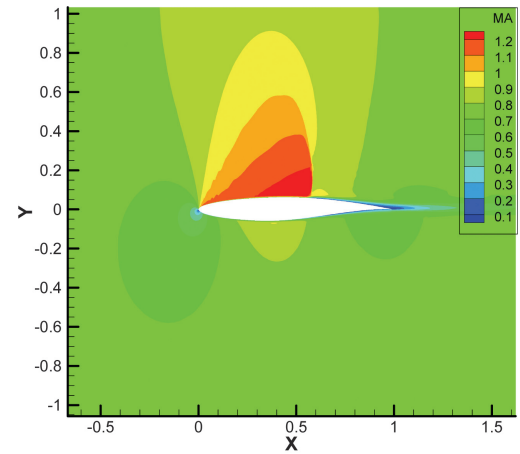
5.1. Transonic flow over the RAE2822 airfoil

The transonic turbulent flow past the RAE2822 airfoil is always seen as a benchmark case for flow solvers. The flow conditions are defined as follows: a Mach number of $M_\infty = 0.75$, a Reynolds number of $Re_\infty = 6.2 \times 10^6$, and an incidence angle of $\alpha = 2.72^\circ$. An initial uniform mesh of 40×40 cells extending 10 chords away from the body is processed with 10 levels of mesh refinement around the body surface. Three levels of feature-based grid adaption are carried out during the solution procedure. The adapted grid at level 3 has 63400 cells and is displayed in Fig.2a.

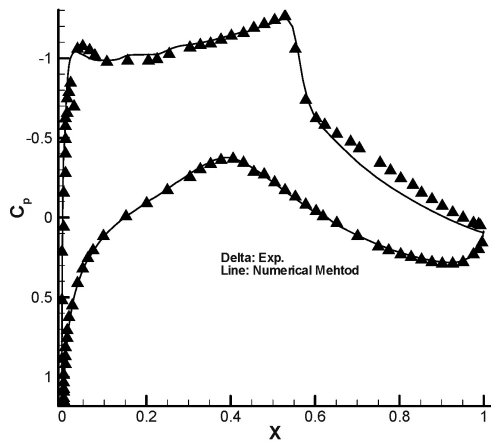
A shock wave on the upper surface and flow separation induced by shock can be seen at this flow conditions. The Mach number contours are shown in Fig 2b, which confirms that the current method has well resolved the high gradient flow features, such as shocks, shear layers. Fig.2c shows a comparison of the surface pressure coefficient (C_p) distribution along the airfoil between the current numerical method and experimental results [23]. The C_p distribution is comparable with the experimental data. Specifically, the shock is sharply captured with a very high resolution. But a slight under-prediction is visible at the at the separated region, this may be caused by the wall function model is not well agreement in the separated region.



a. Feature-adapted mesh



b. Mach contours



c. Comparison of C_p distribution
Fig.2 Results of transonic flow over the RAE2822 airfoil

5.2. Supersonic flow over the circle cylinder

The second case is a supersonic flow over the circle cylinder at freestream Mach number 1.7 and Reynolds number 2.0×10^5 . The computational domain is considered with dimensions $[-10D, 10D] \times [-10D, 10D]$, D being the diameter of the cylinder. The initial computational grid is composed of 9 levels of geometry-based mesh refinements. Fig.3a shows the adapted grid after 3 times of feature-based grid adaption. The Mach number contours are shown in Fig 3b. For the considered freestream Mach number, a bow shock is formed upstream of the cylinder, the subsonic flow at the front stagnation region accelerates to supersonic flow region and envelops a subsonic recirculation region behind the cylinder. Fig.3a and Fig.3b show that the current feature-based grid adaption method can capture shock and shear layer very well. The surface pressure coefficient (C_p) distribution along the cylinder is comparable with the experimental data [24] as shown in Fig.3c. However, the agreement with experimental date is not satisfactory in the recirculation region, this is also caused by the wall function model was used in that region.

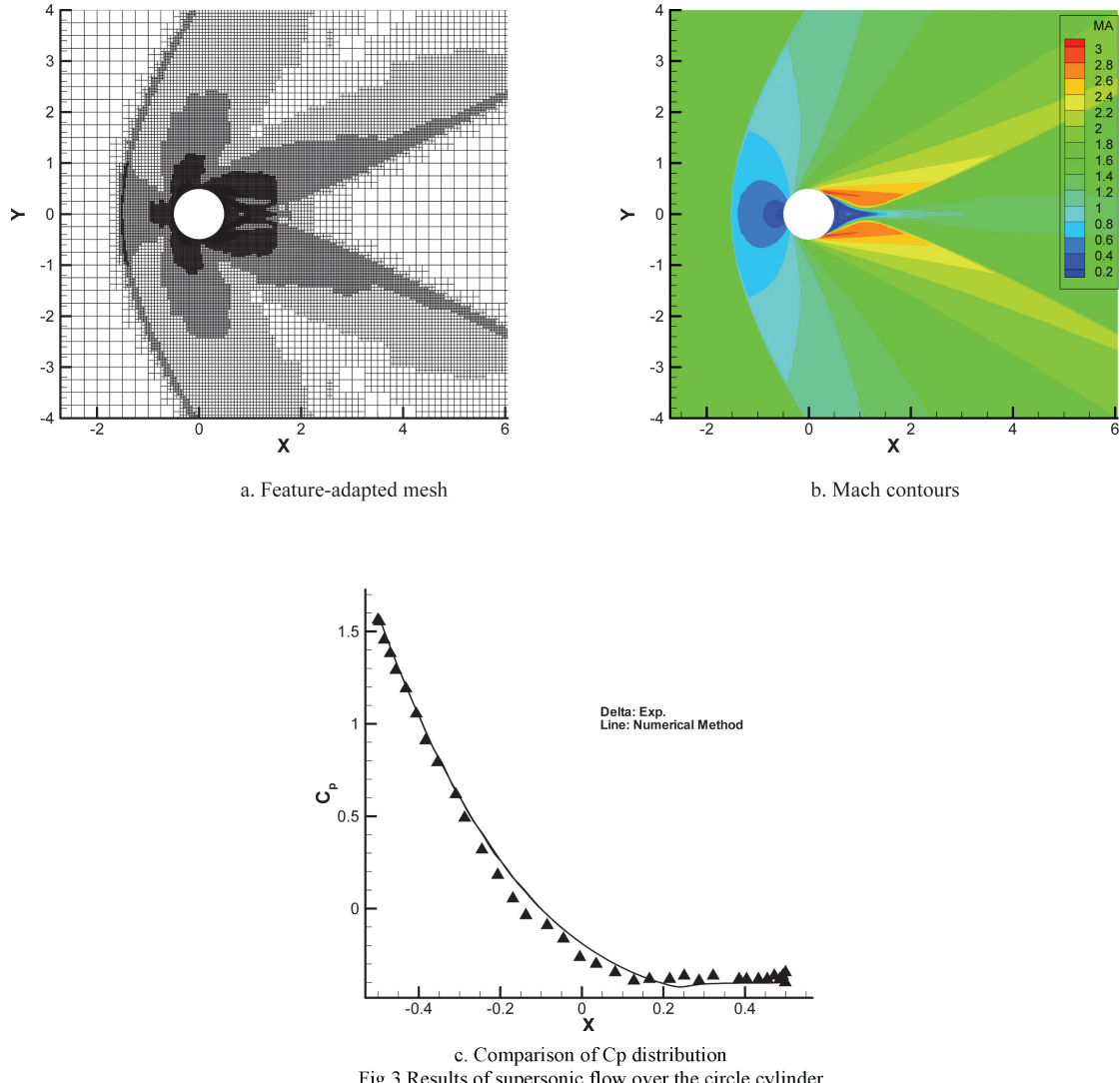


Fig. 3 Results of supersonic flow over the circle cylinder

6. Conclusion

In the present work, a novel non-body-conforming wall boundary treatment method is developed for adaptive Cartesian grids, which referred as “Ghost cell method”. Emphasis was placed in designing new ghost cell turbulent wall boundary conditions for turbulent flows. The wall function model was coupled with the ghost cell method to define the primitive variables and turbulent properties at the ghost cells. Meanwhile, the turbulent variables at the near-wall-cells and boundary cells were modified by using wall function model. Moreover, a feature-based grid adaption improved the solution quality. Numerical simulations were conducted to examine the robustness and accuracy of the present method. The numerical results are found to be comparable with the experimental data. But, the current method had some drawback in dealing with the separated flow problems. This remains a challenging work for future.

Acknowledgement

This research work was supported by the National Natural Foundation of China under Grant 11102179 and 11002071.

References

- [1] De Zeeuw D L, 1993. A Quadtree-Based Adaptively-Refined Cartesian-Grid Algorithm for Solution of the Euler Equations, PhD thesis, University of Michigan.
- [2] Ya'eer Kidron, Yair Mor-Yossef and Yuval Levy, 2009. Turbulent Flow Predictions using a Cartesian Flow Solver, AIAA Paper, 2009-3881.
- [3] Iaccarino G and Verzicco R, 2003. Immersed boundary technique for turbulent flow simulations, *Appl. Mech. Rev.*, Vol. 56, No. 3, p. 331-347.
- [4] Mittal R and Iaccarino G, 2005. Immersed boundary methods, *Annu. Rev. Fluid Mech.*, Vol. 37, p. 239-261.
- [5] Dadone A and Grossman B, 2004. Ghost-Cell Method with far-field coarsening and mesh adaptation for Cartesian Grids, *AIAA Journal*, Vol. 42, No. 12, p. 2499-2507.
- [6] Clarke D, Salas M, and Hassan H, 1986. Euler Calculations for Multi-Element Airfoils using Cartesian Grids, *AIAA Journal*, Vol. 24, p. 1128–1135.
- [7] Marshall D D and Ruffin S M, 2004. An Embedded Boundary Cartesian Grid Scheme for Viscous Flows using a New Viscous Wall Boundary Condition Treatment, AIAA Paper, 2004-581.
- [8] Kupiainen M, Sjögren B, 2009. A Cartesian embedded boundary method for the compressible Navier-Stokes equations, *Journal of Science Computer*, Vol. 41, No. 1, p. 94-117.
- [9] P. De Palma, M.D.de Tullio, Pascazio G and Napolitano M, 2006. An immersed-boundary method for compressible viscous flows, *Computers & Fluids*, Vol. 35, No. 7, p. 693-702.
- [10] M. D. de Tullio, P. De Palma, Iaccarino G, Pascazio G and Napolitano M, 2007. An immersed boundary method for compressible flows using local grid refinement, *Journal of Computer Physics*, Vol. 225, No. 2, p. 2098-2117.
- [11] Toshihiro Kamatsuchi, 2007. Turbulent flow simulation around complex geometries with cartesian grid method, AIAA paper, 2007- 1459.
- [12] Kalitzin G and Iaccarino G, 2002. Turbulence Modeling in an Immersed Boundary RANS Method, CTR Annual Briefs.
- [13] Kalitzin G and Iaccarino G, 2003. Toward immersed boundary simulation of high Reynolds number flows, Center for Turbulence Research Annual Research Briefs 2003, p. 369-378.
- [14] Jae-doo Lee, 2006. Development of an Efficient Viscous Approach in a Cartesian Grid Framework and Application to Rotor-Fuselage Interaction, PhD thesis, University of Michigan.
- [15] F.Capizzano, 2010. A turbulent wall model for immersed boundary methods, AIAA paper, 2010-712.
- [16] Blazek J, 2001. Computational fluid dynamics: principles and applications, Amsterdam: ELSEVIER.
- [17] Sharov D and NaKahashi K, 1997. Reordering of 3-D hybrid unstructured grids for vectorized LU-SGS Navier-Stokes calculations, AIAA Paper, 97-2102.
- [18] Menter F R, 1994. Two-equation eddy-viscosity turbulence models for engineering applications, *AIAA Journal*, Vol. 32, No. 8, p. 1598-1605.
- [19] Liou M S, 1996. A sequel to AUSM: AUSM+, *Journal of Computational Physics*, Vol. 129, No. 2, p. 364-382.
- [20] Nichols R H and Nelson C C, 2004. Wall function boundary conditions including heat transfer and compressibility for transport turbulence models, AIAA Paper, 2004-0581.
- [21] Spalding D B, 1961. A single formula for the law of the wall, *Journal of Applied Mechanics*, Vol. 28, No. 3, p. 455-458.
- [22] O'Rourke J, 1998. Computational geometry in C, Cambridge University Press.
- [23] Cook P H, McDonald M A and Firmin M C P, 1979. Aerofoil RAE2822-Pressure distributions and boundary layer and wake measurements, AGARD Advisory Report AR-138, A6.1-A6.77.
- [24] Bashkin V A , Vaganov A V , Egorov I V , Ivanov D V and Ignatova GA, 2002. Comparison of calculated and experimental data on supersonic flow past a circular cylinder, *Fluid Dynamics 2002*, Vol. 37, No.3, p. 473-483.